

STEEL ELEMENTS WITH TIMBER FIRE PROTECTION - EXPERIMENT AND NUMERICAL ANALYSIS

STANISLAV ŠULC^{a,*}, JAKUB ŠEJNA^b, VÍT ŠMILAUER^a, FRANTIŠEK WALD^b

^a Czech Technical University in Prague, Faculty of Civil Engineering, Department of Mechanics, Thákurova 7, 166 29 Prague 6, Czech Republic

^b Czech Technical University in Prague, Faculty of Civil Engineering, Department of Steel and Timber Structures, Thákurova 7, 166 29 Prague 6, Czech Republic

* corresponding author: stanislav.sulc@fsv.cvut.cz

ABSTRACT. Steel structural elements are sensitive to elevated temperatures, while timber elements have good thermal insulation properties. Timber material can fulfill the role of fire protection of steel members. The effect of the protection is demonstrated on an experiment with three beams with different levels of the protection, placed into a horizontal furnace. The experimental task was also numerically analysed with standard computational approach given by the Eurocode [1, 2], which leads to an interesting comparison, as the calculation is supposed to provide higher temperatures and larger deformations compared to the experimental data.

KEYWORDS: Timber, fire protection, fire resistance, furnace experiment.

1. INTRODUCTION

Steel structural elements are very sensitive to elevated temperatures [3, 4], which leads to protecting them with methods as fire protective paints or panel lining [5]. The protection can also fulfill the visual design demands, which sometimes leads to using timber panels or beams to cover the steel elements. Although timber itself can serve as a fuel, its thermal insulating properties and low charring rate can effectively delay the effect of the surrounding fire load, and for some time it can be effectively taken as a fire protection [6, 7].



FIGURE 1. Beams in the furnace during the experiment.

This article presents an experimental comparison of beam elements with different levels of fire protection using timber panel lining made of OSB panels. The beams, placed in a horizontal furnace, were also mechanically loaded to represent a real example of use and to study the mechanical behaviour. This article presents a comparison of the experimental data with

simulations based on material models defined by the Eurocode [1, 2].

2. DESCRIPTION OF THE EXPERIMENT

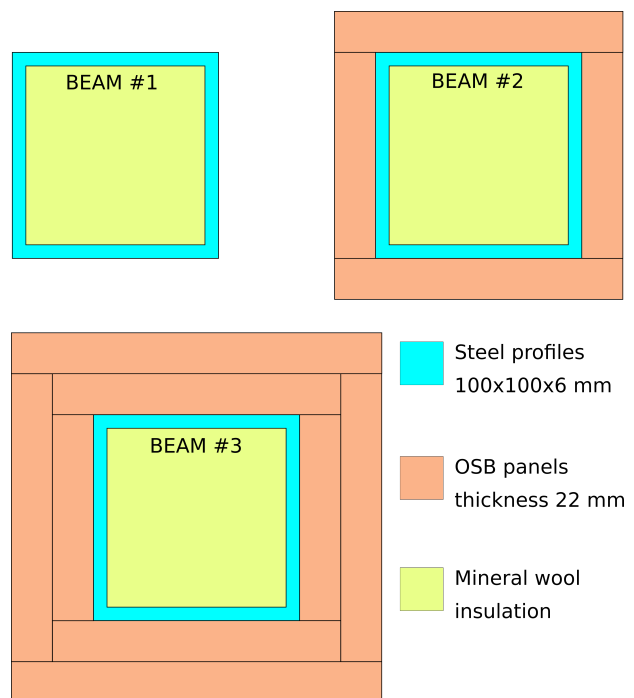


FIGURE 2. Cross sections of the beams.

The subjects of study were three steel beams with outer dimension 100×100 mm and thickness of 6 mm, placed in a horizontal furnace. The steel type was S235. Beam #1 had no protection against fire, beam #2 was protected with one layer of 22 mm OSB panels, and beam #3 was protected with two of these layers,

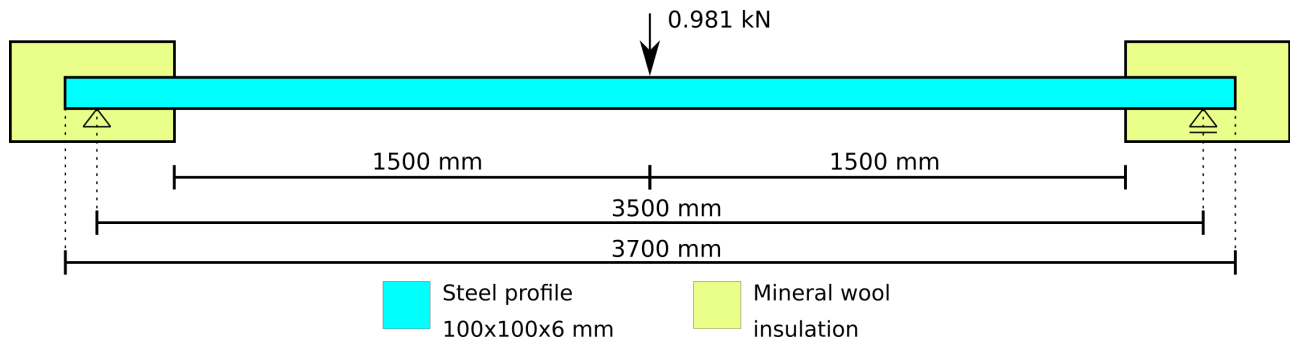


FIGURE 3. Geometry of the task, depicted unprotected beam.

see the cross sections in Fig. 2 and the photo in Fig. 4. The span length was 3.5 m and the beams were loaded with 100 kg in the middle. See the geometry in Fig. 3.

The OSB panels were connected to each other with 50 mm narrow crown staples, which are commonly used for OSB panels, see Fig. 4, so the integrity of the beam should be the same as in a real application.

The furnace was heated with eight gas burners and the temperature regulation followed the ISO 834 temperature curve given by the Eurocode 5 [2].

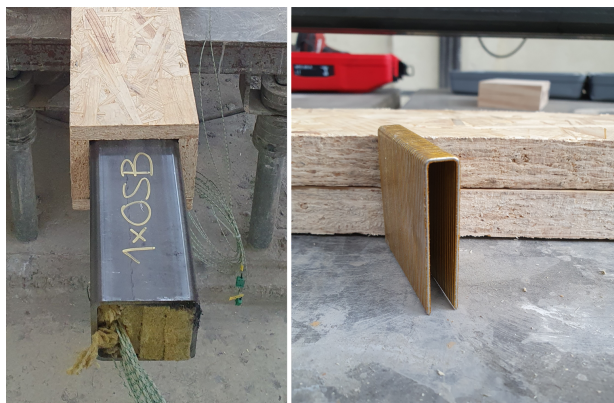


FIGURE 4. Photo of the beam #2 with one layer of OSB protection (left) and the 50 mm narrow crown staples (right).

The temperatures of steel were measured with thermocouples and the adiabatic surface temperatures were measured by plate thermometers positioned close to the beams. Each beam's vertical displacement was measured in the middle of its span.

3. RESULTS OF THE EXPERIMENT

The temperatures from the middle of the span of each beam are presented in Fig. 5. It clearly shows the effect of the timber protective layer, which causes slower temperature increase according to the thickness of the layer. Approximately at the time of 25 minutes the timber panels fell off completely from beam #2, which causes the rapid temperature increase. This happened for beam #3 approximately at the time of 45 minutes. The falling off of the panels is partially caused by the mechanical loading of the beams. The

time of falling off cannot be predicted precisely, as it is rather a probability task to define how long time the panels keep protecting the beams, which cannot be defined by one experiment.

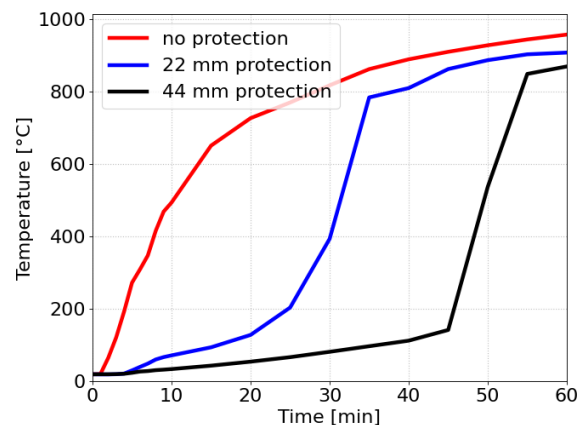


FIGURE 5. Temperature comparison of the unprotected and protected steel beams.

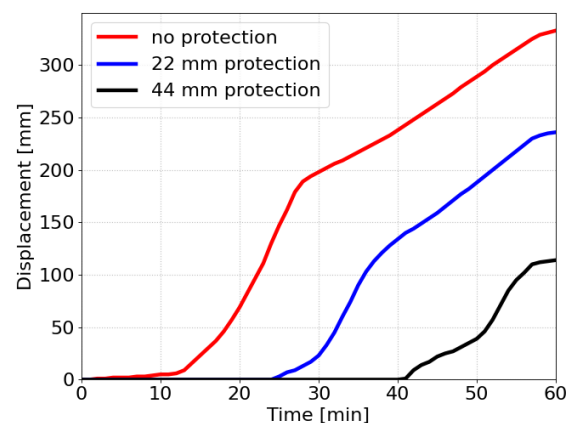


FIGURE 6. Displacement comparison of the unprotected and protected steel beams.

Fig. 5 presents that adding one layer of the OSB panels causes approximately 20 minutes delay of the temperature increase, which is a very satisfying effect of the protection. The difference is also clearly expressed by displacements in Fig. 6.

4. NUMERICAL SIMULATIONS

We present numerical simulations of the experiment to show the capabilities of standard computational approach based on material properties and models from the EC3 [1] and EC5 [2] documents.

4.1. THERMAL TASK

The thermal task calculates temperature of the steel beam in the middle of its span, as there the data is least affected by the beam endings. The boundary conditions are defined by the adiabatic surface temperature, measured by plate thermal sensors, which provided almost identical values as the prescribed ISO 834 time-temperature curve. The surface emissivity and heat transfer coefficient were assumed as 0.95 and 20 W/m/K.

The temperature-dependent functions of timber thermal conductivity, specific heat capacity and bulk density are depicted in Figs. 7, 8 and 9. The values conservatively assume 0 % initial moisture content.

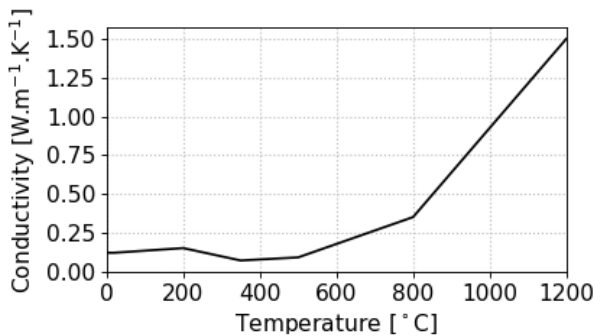


FIGURE 7. EC5 timber thermal conductivity.

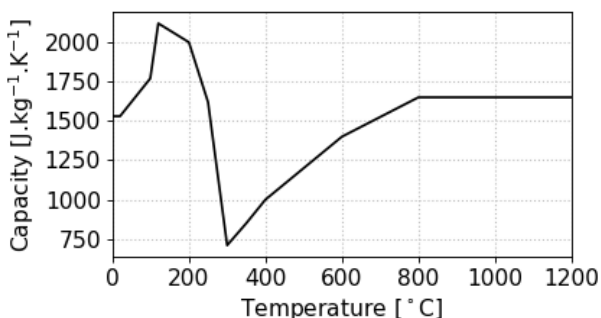


FIGURE 8. EC5 timber specific heat capacity.

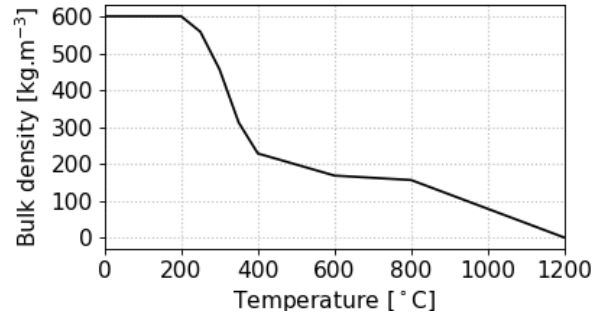


FIGURE 9. EC5 timber bulk density.

Bulk density of steel was considered as 7850 kg/m³. Temperature-dependent functions of thermal conductivity and specific heat capacity are depicted in Figs. 10 and 11.

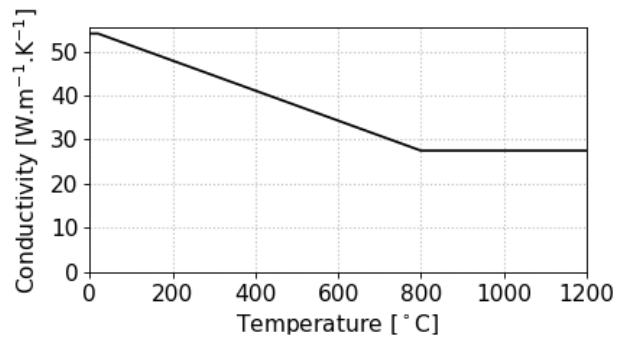


FIGURE 10. EC3 Steel thermal conductivity.

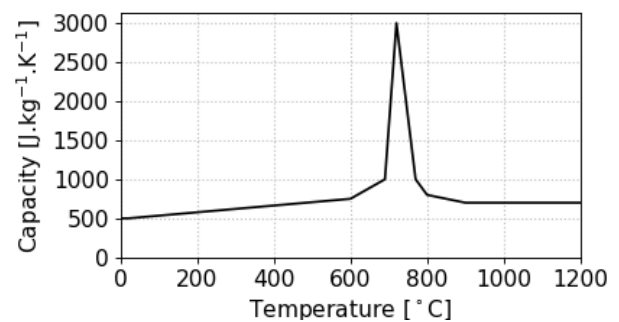


FIGURE 11. EC3 Steel specific heat capacity.

4.1.1. RESULTS

Fig. 12 shows that in case of beam #1 the simulation results match the experimental data very well, which confirms that the computation is properly defined and the task without OSB protection is very well predictable.

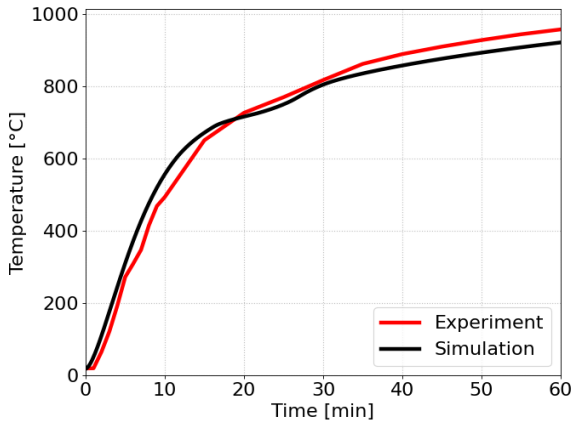


FIGURE 12. Comparison of experimental and simulated temperatures for the unprotected beam.

The results on beams #2 and #3, depicted in Figs. 13 and 14, show a comparison of results with basic timber model and this model with modification for the OSB material. As the EC5 defines the temperature-dependent functions of thermal conductivity, specific heat capacity and bulk density of plain timber, these function are not defined for OSB material. But it provides the charring rate for both timber (0.65 mm/min) and OSB (0.9 mm/min) for equal conditions. The conductivity function was multiplied by the ratio of these two values, which lead to the results denoted by blue lines, which are closer to the experimental data, but still underestimating the temperature.

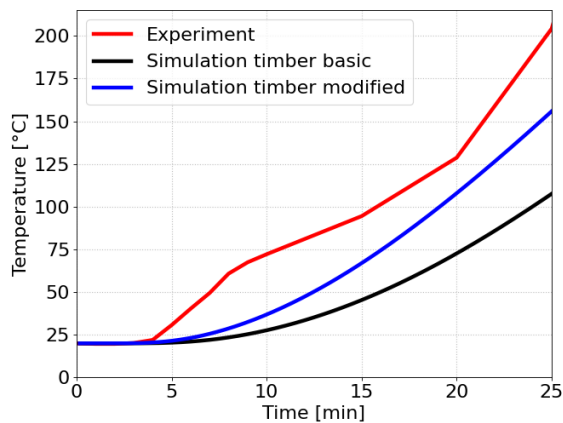


FIGURE 13. Comparison of experimental and simulated temperatures for beam protected with 22 mm OSB panels until the time when the protection fell off.

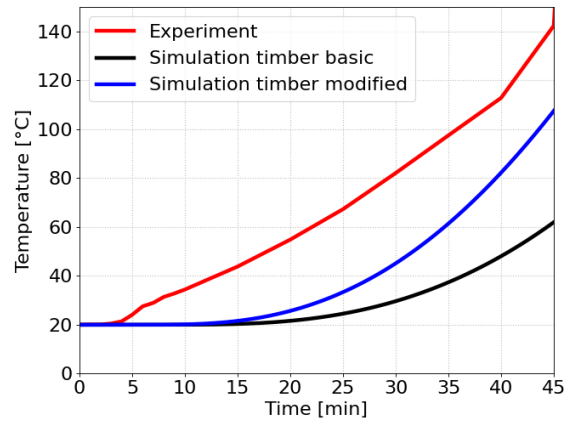


FIGURE 14. Comparison of experimental and simulated temperatures for beam protected with two layers of 22 mm OSB panels until the time when the protection fell off.

The EC5 timber thermal model is working well for the charring rate propagation through the timber itself under the conditions of the ISO-834 time-temperature curve, but it seems that when we change some boundary conditions, the accuracy of the model is not that good, as it changes the task definition significantly.

4.2. MECHANICAL TASK

The key input for the mechanical task is the temperature field, which reduces the mechanical properties. Here we consider the temperatures which were measured during the experiment to avoid negative influence coming from the thermal task imperfections.

The mechanical behavior given by the EC3 document is defined by the diagram in Fig. 15. The effective yield strength function $\sigma_{y,\theta}$ is depicted in Fig. 16 and the proportional limit function $\sigma_{p,\theta}$ is depicted in Fig. 17. The starting linear part is given by the Young's modulus function $E_{a,\theta} = \tan(\alpha)$, which is depicted in Fig. 18. The strain parameter $\varepsilon_{y,\theta} = 0.02$, $\varepsilon_{t,\theta} = 0.15$ and $\varepsilon_{u,\theta} = 0.2$.

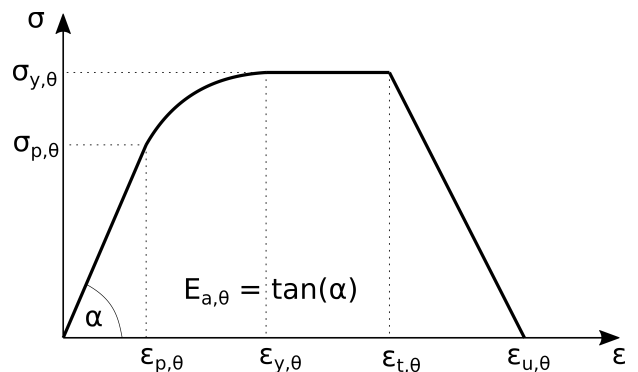


FIGURE 15. Considered strain-stress diagram of steel, given by EC3.

The curved part of the stress function is defined as

$$\sigma(\varepsilon) = \sigma_{p,\theta} - c + \frac{b}{a} \sqrt{a^2 - (\varepsilon_{y,\theta} - \varepsilon)^2} \quad (1)$$

where

$$c = \frac{(\sigma_{y,\theta} - \sigma_{p,\theta})^2}{(\varepsilon_{y,\theta} - \varepsilon_{p,\theta})E_{a,\theta} - 2(\sigma_{y,\theta} - \sigma_{p,\theta})} \quad (2)$$

$$b = \sqrt{c(\varepsilon_{y,\theta} - \varepsilon_{p,\theta})E_{a,\theta} + c^2} \quad (3)$$

$$a = \sqrt{(\varepsilon_{y,\theta} - \varepsilon_{p,\theta})(\varepsilon_{y,\theta} - \varepsilon_{p,\theta} + \frac{c}{E_{a,\theta}})} \quad (4)$$

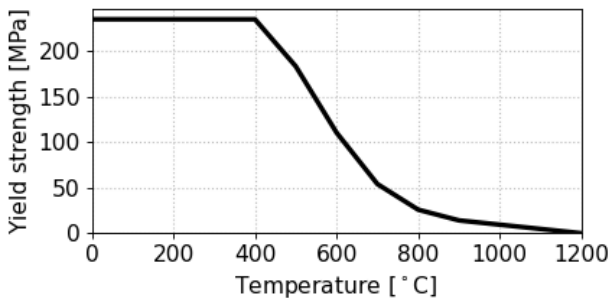


FIGURE 16. Temperature-dependent effective yield strength of steel, given by EC3.

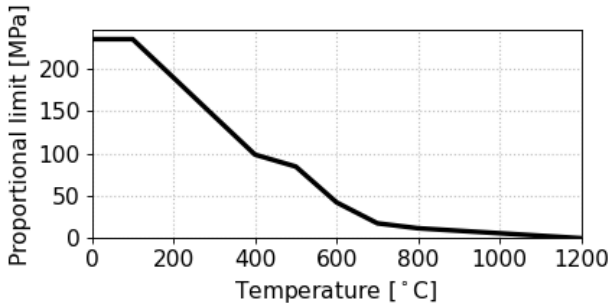


FIGURE 17. Proportional limit of steel, given by EC3.

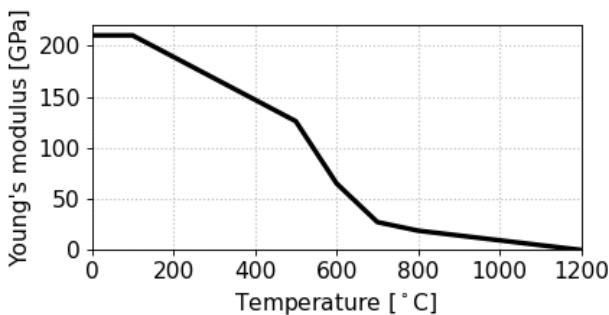


FIGURE 18. Temperature-dependent young's modulus of steel, given by EC3.

4.2.1. RESULTS

The displacement results are presented and compared with experimental data in Figs. 19, 20 and 21. It

shows that the mechanical behaviour of steel changes significantly after reaching the temperature 600 °C.

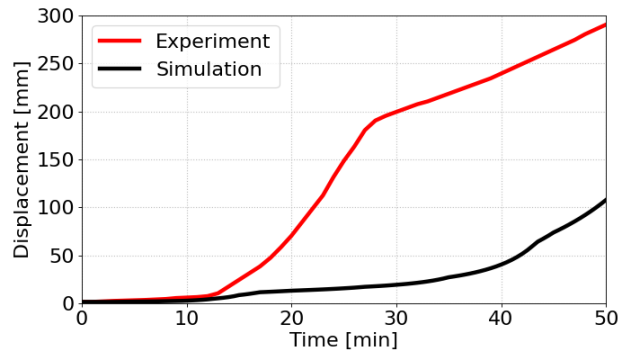


FIGURE 19. Comparison of the experimental and calculated displacements for beam #1.

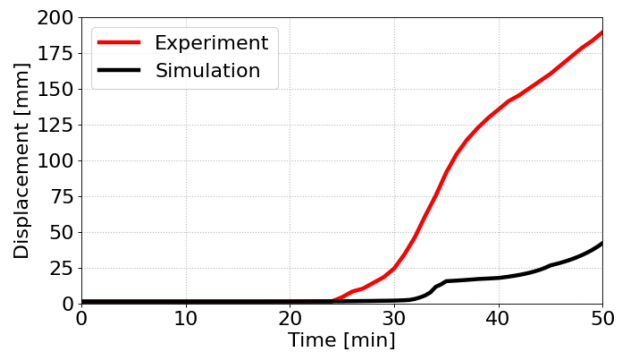


FIGURE 20. Comparison of the experimental and calculated displacements for beam #2.

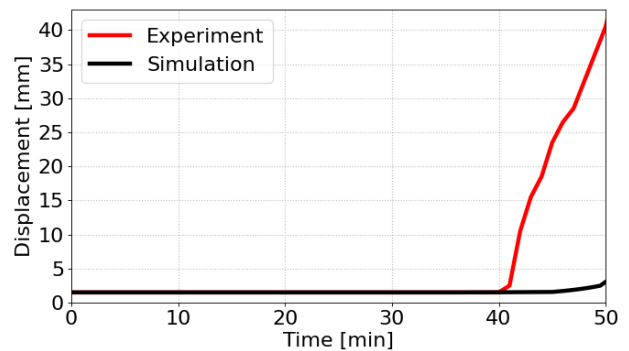


FIGURE 21. Comparison of the experimental and calculated displacements for beam #3.

The results also show that during all the time the displacements calculated by the EC3 methodology are much smaller than those measured during the experiment, which is caused by the high-temperature steel creep behaviour. This time-dependent phenomenon is missing in the EC3 mechanical model, which corresponds with the data summarization by Wald et al. [8]. EC3 defines the material behaviour for the temperature range up to 1200 °C, but it seems to be valid only for short-time applied load.

It is more complicated to predict the mechanical behaviour above 600 °C, the behaviour is often studied only below this temperature, as the EC3 also limits the fire-resistance by temperature. Fig. 22 presents the displacement on beam #1 before the temperature reached 600 °C, which is not well visible in Fig. 19. It shows that the creep behaviour for these lower temperatures and time of several minutes is also significant in the relative comparison.

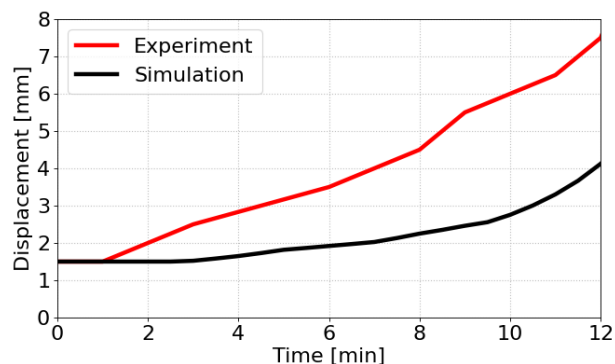


FIGURE 22. Comparison of the experimental and calculated displacements for beam #1 until reaching the temperature of 600 °C.

5. CONCLUSIONS

The experiment proved that it is reasonable to use timber as a fire-protection, as it provides good thermal insulation and is present long enough to work as a retardant of the thermal load.

The comparison of the calculated and experimental data showed underestimating of temperatures, as the thermal material model of timber from EC5 doesn't work perfectly for our task where timber serves as a fire-protective layer in combination with the steel material, although it performs well in tasks where the whole domain is made of timber. It also showed that the steel material behaviour defined in the EC3 doesn't take steel creep time-dependent behaviour into account, as there occurs a significant difference for the displacements, which agrees with other existing studies.

This article brings experimental data for high temperatures above 600 °C, which will be used for development and validation of creep material models in our future work, as there is the need to find an easy-usable model which could be safely used for calculations to estimate the conservative fire resistance of structures where the time plays a non-negligible role.

ACKNOWLEDGEMENTS

This research was funded by Czech Science Foundation, grant 19-22435S “Performance of structures with timber fire protection—multi-physics modelling”, and also by Czech Technical University in Prague, grant number SGS21/037/OHK1/1T/11.

REFERENCES

- [1] EN 1993-1-2:2006, Eurocode 3: Design of steel structures - Part 1-2: General rules - Structural fire design, 2005.
- [2] EN 1995-1-2:2006, Eurocode 5: Design of timber structures - Part 1-2: General - Structural fire design, 2006.
- [3] G. Li, P. Wang. Properties of steel at elevated temperatures. *Advanced Analysis and Design for Fire Safety of Steel Structures* 2013. https://doi.org/10.1007/978-3-642-34393-3_3.
- [4] Z. Nie, Y. Li, Y. Wang. Mechanical properties of steels for cold-formed steel structures at elevated temperatures. *Advances in Civil Engineering* 2020.
- [5] S. Gnanachelvam, A. Ariyanayagam, M. Mahendran. Fire resistance of light gauge steel framed wall systems lined with pcm-plasterboards. *Fire Safety Journal* **108**:102838, 2019. <https://doi.org/10.1016/j.firesaf.2019.102838>.
- [6] D. H. L. Truong, T. Meng-Ting. Experimental assessment of the fire resistance mechanisms of timber-steel composites. *MDPI - Materials* 2019. <https://doi.org/10.3390/ma12234003>.
- [7] F. Riola-Parada, K. Tavoussi, A. Fadai, et al. Fire performance of prefabricated timber-steel-concrete ribbed decks. In *Conference: WCTE 2018 - World Conference on Timber Engineering*. Seoul, South Korea, 2018.
- [8] F. Wald, I. Burgess, L. Kwasniewski, et al. Benchmark studies - Experimental validation of numerical models in fire engineering. *CTU Publishing House, Czech Technical University in Prague* 2014.